NASA-TM-112538

Chemical Loss of Ozone in the Arctic Polar Vortex in the Winter of 1991–1992

R. J. Salawitch, S. C. Wofsy, E. W. Gottlieb, L. R. Lait, P. A. Newman, M. R. Schoeberl, M. Loewenstein, J. R. Podolske, S. E. Strahan, M. H. Proffitt, C. R. Webster, R. D. May, D. W. Fahey, D. Baumgardner, J. E. Dye, J. C. Wilson, K. K. Kelly, J. W. Elkins, K. R. Chan, J. G. Anderson

In situ measurements of chlorine monoxide, bromine monoxide, and ozone are extrapolated globally, with the use of meteorological tracers, to infer the loss rates for ozone in the Arctic lower stratosphere during the Airborne Arctic Stratospheric Expedition II (AASE II) in the winter of 1991–1992. The analysis indicates removal of 15 to 20 percent of ambient ozone because of elevated concentrations of chlorine monoxide and bromine monoxide. Observations during AASE II define rates of removal of chlorine monoxide attributable to reaction with nitrogen dioxide (produced by photolysis of nitric acid) and to production of hydrochloric acid. Ozone loss ceased in March as concentrations of chlorine monoxide declined. Ozone losses could approach 50 percent if regeneration of nitrogen dioxide were inhibited by irreversible removal of nitrogen oxides (denitrification), as presently observed in the Antarctic, or without denitrification if inorganic chlorine concentrations were to double.

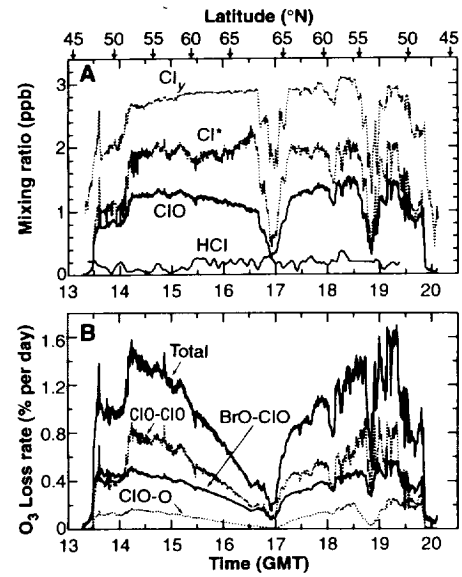

Fig. 1. Observations and reconstructions for 20 January 1992. (**A**) Observed mixing ratios of ClO and HCl, inferred mixing ratios for Cl* and Cl_y, and (**B**) the 24-hour mean loss rates for ozone, computed using Eq. 4 and Cl* shown in (A). The total recombination rate and contributions from the ClO-ClO, BrO-ClO, and ClO-O catalytic cycles (reactions 1, 2, and 3) are shown. All measurements taken along the ER-2 flight track, plotted against universal time (GMT). Corresponding latitudes are indicated at the top of the figure.

Loss rates for O_3 were estimated for the lower stratosphere during AASE II in 1991–1992. We computed distributions of reactive chlorine ($Cl^* \equiv [ClO] + 2 \times [(ClO)_2]$) and bromine ($Br^* \equiv [BrO] + [BrCl]$) (where brackets denote concentration) along the flight track of the ER-2 airplane by assimilating in situ observations of ClO and BrO with a simple model. Relations between potential vorticity (PV) and potential temperature (Θ), meteorological tracers (*1*, *2*), and Cl* and Br* were developed to compute O_3 loss rates for the north polar region, accounting for the influence of insolation, temperature, and pressure as air circulates around the polar vortex (*3*, *4*). Seasonal changes observed for ClO (*5*), NO (*6*), HCl (*7*), and O_3 (*8*) were investigated with the use of a photochemical model constrained by meteorological observations (*9*) and measured surface areas for sulfate aerosol (*10*); factors regulating chemical removal of O_3 in the Arctic were examined with this model.

Reactions on the surfaces of polar stratospheric clouds (PSCs) (*11*), which are composed of condensed phases of H_2O and HNO_3 (*12*), catalyze the rapid conversion of HCl and $ClNO_3$ to labile species of inorganic chlorine in the polar vortex during winter (*13*, *14*). Three catalytic cycles involving halogens account for ~95% of photochemical loss of O_3 in the vortex.

1) The self-reaction of ClO forming its dimer, $(ClO)_2$, followed by photolysis

$$ClO + ClO + M \rightarrow (ClO)_2 + M \quad (1)$$
$$(ClO)_2 + h\nu \rightarrow ClOO + Cl$$
$$ClOO \rightarrow Cl + O_2$$
$$2(Cl + O_3 \rightarrow ClO + O_2)$$
$$\text{Net: } 2O_3 \rightarrow 3O_2$$

catalyzes the recombination of two O_3 molecules with the use of one photon (with energy $h\nu$) (*15*). Thermal decomposition of $(ClO)_2$ short-circuits this cycle, regenerating ClO without producing Cl atoms or recombining O_3.

2) The reaction of BrO and ClO and the photolysis of BrCl

$$BrO + ClO \rightarrow Cl + Br + O_2 \quad (2a)$$
$$\rightarrow Br + OClO \quad (2b)$$
$$\rightarrow BrCl + O_2 \quad (2c)$$
$$BrCl + h\nu \rightarrow Br + Cl$$
$$Br + O_3 \rightarrow BrO + O_2$$
$$Cl + O_3 \rightarrow ClO + O_2$$
$$\text{Net (2a, 2c): } 2O_3 \rightarrow 3O_2$$

also catalyzes recombination of O_3 (*13*). Photolysis of OClO produces O atoms; therefore, reaction 2b does not destroy O_3 (*16*).

3) The reaction sequence

R. J. Salawitch, S. C. Wofsy, E. W. Gottlieb, Division of Applied Sciences and Department of Earth and Planetary Sciences, Harvard University, Cambridge, MA 02138.
L. R. Lait, P. A. Newman, M. R. Schoeberl, S. E. Strahan, National Aeronautics and Space Administration (NASA) Goddard Space Flight Center, Greenbelt, MD 20771.
M. Loewenstein, J. R. Podolske, K. R. Chan, NASA Ames Research Center, Moffett Field, CA 94035.
M. H. Proffitt, D. W. Fahey, K. K. Kelly, National Oceanic and Atmospheric Administration (NOAA) Aeronomy Laboratory, Boulder, CO 80303.
C. R. Webster and R. D. May, Jet Propulsion Laboratory, Pasadena, CA 91109.
D. Baumgardner and J. E. Dye, National Center for Atmospheric Research, Boulder, CO 80307.
J. C. Wilson, Department of Engineering, University of Denver, Denver, CO 80208.
J. W. Elkins, NOAA Climate Monitoring and Diagnostics Laboratory, Boulder, CO 80303.
J. G. Anderson, Departments of Earth and Planetary Sciences and Chemistry, Harvard University, Cambridge, MA 02138.

NASA-TM-112501

Reprint Series
27 August 1993, Volume 261, pp. 1146–1149

SCIENCE

Chemical Loss of Ozone in the Arctic Polar Vortex in the Winter of 1991–1992

R. J. Salawitch, S. C. Wofsy, E. W. Gottlieb, L. R. Lait, P. A. Newman, M. R. Schoeberl, M. Loewenstein, J. R. Podolske, S. E. Strahan, M. H. Proffitt, C. R. Webster, R. D. May, D. W. Fahey, D. Baumgardner, J. E. Dye, J. C. Wilson, K. K. Kelly, J. W. Elkins, K. R. Chan, and J. G. Anderson

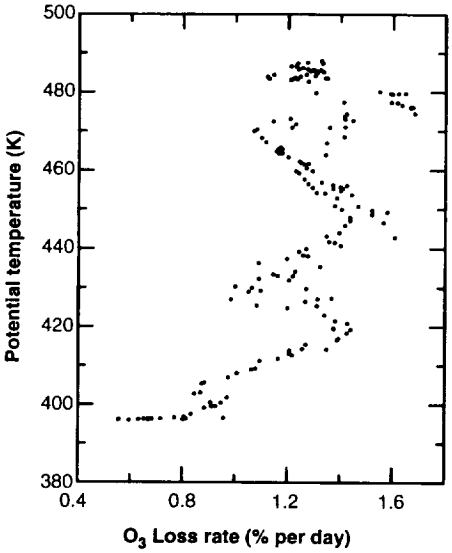

Fig. 2. The 24-hour mean loss rates for O_3 plotted against potential temperature Θ, for observations taken on 20 January 1992 during the descent and ascent in sunlight (solar zenith angle <80°) at 52°N. The altitudes 20, 16, and 15 km correspond approximately to Θ = 500, 420, and 400 K, respectively.

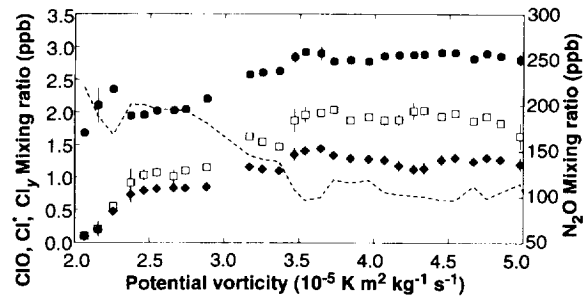

Fig. 3. Observed mixing ratios for ClO (◆) and N_2O (dashed line) and inferred mixing ratios for Cl* (□) and Cl_y (●) on the isentropic surface defined by Θ = 470 ± 10 K, plotted against potential vorticity (PV). Data were averaged in intervals of PV equal to 5 × 10^{-7} K m^2 kg^{-1} s^{-1}. The edge of the polar vortex was located at PV ≈ 2.1 × 10^{-5} with a transition region between 2.3 × 10^{-5} and 3 × 10^{-5} K m^2 kg^{-1} s^{-1}. The interior of the vortex had uniform concentrations of Cl_y ≈ 2.8 ppbv and Cl*/Cl_y ≈ 0.75. Vertical bars denote standard deviation (smaller than the symbol in many bins).

$$\begin{aligned} ClO + O &\rightarrow Cl + O_2 \qquad (3)\\ Cl + O_3 &\rightarrow ClO + O_2\\ \text{Net: } O + O_3 &\rightarrow 2O_2 \end{aligned}$$

represents a minor loss of O_3, with rates accelerating in spring when the concentration of O atoms increases.

Hydrolysis of N_2O_5 on sulfate aerosols efficiently converts NO_x ($NO + NO_2$) to HNO_3, which is very stable at low sun angles (*6*, *17*). Catalytic cycles involving NO_x, normally important at mid-latitudes, are negligible in the winter polar stratosphere (*18*). The catalytic cycle involving reaction of ClO with HO_2 represents less than 5% of the total loss of O_3 [on the basis of calculated values for HO_2, corroborated by column measurements of HOCl (*19*)] and is therefore not considered here.

The photochemical loss rate of ozone is

$$\frac{d[O_3]}{dt} = -2\{k_{ClO+ClO}R[M][ClO]^2 + (k_{ClO+BrO(a)} + k_{ClO+BrO(c)})[BrO][ClO] + k_{O+ClO}[O][ClO]\} \qquad (4)$$

where k is the rate coefficient for the specified reaction, M denotes an air molecule, and R is

$$\frac{J_{(ClO)_2}[(ClO)_2]}{J_{(ClO)_2}[(ClO)_2] + k_{(ClO)_2+M}[M][(ClO)_2]}$$

the fraction of $(ClO)_2$ that photolyzes, where J is the photolysis frequency for the specified reaction. Removal rates attributable to reaction 1 decline at temperatures above 220 K, where $R \rightarrow 0$ (*20*). Loss of O_3 requires sunlight to photolyze $(ClO)_2$, BrCl (the nighttime reservoir for BrO), and O_3 (to generate O atoms).

Equation 4 allows us to compute instantaneous rates for O_3 loss along a flight track directly from measured radicals (*5*, *21*), apart from R and [O], which are calculated with Eqs. 5 and 7 below. To determine global loss rates of O_3, we must infer radical concentrations throughout the polar vortex from observations along the flight track, and the loss rate must be integrated over 24 hours (*3*).

The diurnal variations of ClO, BrO, and O are governed by

$$\frac{d[ClO]}{dt} = 2\{J_{(ClO)_2} + k_{(ClO)_2+M}[M]\}[(ClO)_2] - 2k_{ClO+ClO+M}[M][ClO]^2 \qquad (5)$$

$$\frac{d[BrO]}{dt} = J_{BrCl}[BrCl] - k_{ClO+BrO(c)}[BrO][ClO] \qquad (6)$$

$$\frac{d[O]}{dt} = J_{O_3}[O_3] - k_{O+O_2+M}[O][O_2][M] \qquad (7)$$

Equation 5 balances production and loss of $(ClO)_2$, Eq. 6 balances production and photolysis of BrCl, and Eq. 7 balances photolysis of O_3 with recombination of O and O_2; each process has a relaxation time shorter than 1000 s. We determined the concentration of reactive chlorine corresponding to each measurement of ClO by matching observations to diurnal calculations with Eq. 5. Concentrations of BrO were about twice as high inside the vortex than outside, with little change during the winter; hence, a fixed relation was adopted between Br* and Θ (*22*).

Concentrations of ClO began to increase dramatically in late December after temperatures over Asia had cooled to the threshold for PSCs (*5*, *9*). Concentrations of ClO peaked in late January and then declined slowly in February and March. On 20 January 1992, the ER-2 aircraft departed Bangor, Maine (44°47′N, 68°47′W), at 1300 GMT, flew north at ~18-km altitude (Θ = 460 K), and turned south to return at ~19 km (Θ = 490 K), with brief descents to 15 km at 65° and 52°N. Figure 1A shows data for ClO and HCl and inferred values of Cl* and total inorganic chlorine, Cl_y [computed from observations of N_2O and organochlorine gases (*23*)]. A steep decline in N_2O and an increase in ClO were observed just north of Bangor (Fig. 1A) at the edge of the polar vortex (PV ≈ 2.1 × 10^{-5} K m^2 kg^{-1} s^{-1}). Mixing ratios for ClO rose to 0.8 parts per billion by volume (ppbv) (1 ppbv = 10^{-9} mole fraction in air) near the vortex edge, increasing to 1.2 to 1.4 ppbv further inside; less than 15% of Cl_y was converted to Cl* outside the vortex, 60% near the edge, and 75 to 85% in the interior (*24*). Figure 1B shows loss rates of ozone along the flight track, computed by integrating Eq. 4 over 24 hours. Removal rates exceeded 1.4% per day: 50% attributed to reaction 1, 35% to 2, and 15% to 3.

Ozone loss rates in the polar vortex (Fig. 2) were uniform for 420 < Θ < 500 K (16 to 20 km), declining at lower Θ. The mixing ratios of ClO, Cl*, Cl_y, and N_2O versus PV for Θ = 470 ± 10 K are shown in Fig. 3. Monotonic increases of the Cl* value on an isentropic (constant Θ) surface were derived for 8 of the 10 flights in the vortex; similar values for Cl* were observed for a given PV on flights a few days apart. These results imply a homogeneous distribution for Cl* in the polar vortex, extending over more than 4 km in the vertical and as far north as 70°N. Values of Cl* versus PV were similar in 1989 and 1992 (*3*).

We computed distributions of Cl* and daily loss rates for O_3 throughout the vortex using global meteorological fields for PV and the observed relation between Cl* and PV (Fig. 4). Regions with elevated Cl* were exposed to sunlight in lobes of the vortex that extended to 45°N, one of which was sampled by the ER-2. The mean ozone loss rate for the vortex region (PV > 2.1 × 10^{-5} K m^2 kg^{-1} s^{-1}) was 0.4% per day, notably lower than rates along the flight track (Fig. 1B). This difference illustrates the importance of assimilating aircraft observations in a tracer model to account for distortion of the polar vortex from axial symmetry (*2*, *3*). Ozone loss rates found here are similar to those inferred from

measurements of ClO in the Arctic lower stratosphere made between 1 and 13 January 1992 by the Microwave Limb Sounder on the Upper Atmosphere Research Satellite (*25*).

After 1 February, minimum temperatures in the vortex exceeded the threshold for PSCs (*5, 9*), ending PSC processing. Little or no denitrification was observed (*26*), and Cl* and rates for ozone destruction began to decline (Fig. 5). The influence of illumination is evident in Fig. 5B: Loss rates were larger for given Cl* at lower latitudes (lower PV). However, elevated Cl* persisted longer at high latitudes, and O_3 losses integrated over the winter were similar for a wide range of latitudes. About 0.7 part per million by volume (ppmv) (1 ppmv = 10^{-6} mole fraction in air) of O_3 (~15 to 20%) was removed by reactions 1 through 3 at $\Theta = 470 \pm 10$ K in the Arctic polar vortex in 1991–1992, similar to losses for 1988–1989 (*3, 27*).

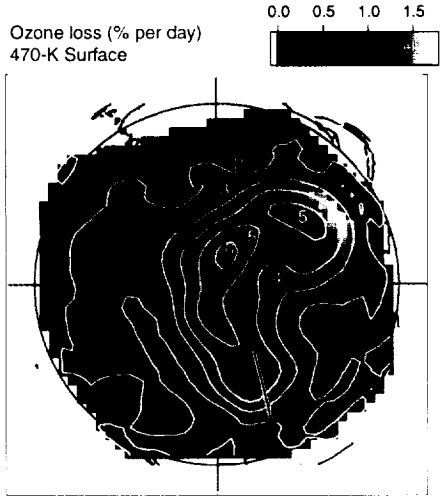

Fig. 4. Distribution of the 24-hour mean loss rate for O_3 (percent per day) in the north polar vortex for the 470 ± 10 K isentrope, derived with global fields of PV and the relation between Cl* and PV shown in Fig. 3, as described in the text. Contours of PV (in units of 10^{-5} K m^2 kg^{-1} s^{-1}) and the flight track of the ER-2 (black line, with circle denoting Bangor, Maine) are shown. Latitude circles 60° and 30°N and a map of the continents are denoted by green lines.

Table 1. Photochemical model results for ozone loss at 18 km.

Case	Model conditions	O_3 removal* (%)
A	PSCs every 8 days until 25 January	19
B	PSCs every 8 days until 26 February	26
C	Case A plus 90% denitrification at first PSC event	44
D	Case A plus twice the present Cl_y	48

*Stated relative to a model without PSCs (see Fig. 6).

The ozone loss rates in Fig. 5B represent snapshots of an isentropic surface on which air parcels move adiabatically (*28*). Nonadiabatic processes, such as radiative cooling, can significantly modify PV and Θ over time scales of a month, with changes in Θ of about −70 K over the winter (*29*). The seasonal integral at $\Theta = 470$ K nevertheless may approximate net ozone removal at ~18 km because O_3 loss rates are uniform in both vertical ($420 < \Theta < 500$ K) (Fig. 2) and horizontal (Fig. 5B) dimensions. Transport of O_3 to $\Theta = 470$ K during the winter makes it difficult to detect net chemical removal of 0.7 ppmv (*8*). Analysis of temporal variations of N_2O and O_3 suggest reduction of 15 to 20% of O_3 at 17 km (*8*) and 10 to 15% between 10 and 12 km (*30*), consistent with chemical loss rates computed here.

Season-long observations during AASE II provide a unique opportunity to test ideas about the photochemical processes regulating radical concentrations in the polar vortex. We calculated production and loss of O_3 and the evolution of ClO, HCl, NO, and BrO from 15 December 1991 to 30 March 1992 for a hypothetical air parcel at $\Theta = 470$ K, 65°N (PV ≈ 2.8×10^{-5} K m^2 kg^{-1} s^{-1}), assumed to circulate around the vortex every 8 days, by solving time-dependent equations (*31*) with a comprehensive set of chemical reactants, reaction rates, and photolysis cross sections (*20*). Data from the ER-2 in December were adopted to define initial concentrations of total nitrogen oxides (NO_y) (*6*), HCl (*7*), O_3 (*8*), H_2O, CH_4, temperature (*9*), and the surface area of sulfate aerosols (*10*) on 15 December. Values of Cl_y were inferred from measured N_2O (*23, 26*). The reaction efficiency for hydrolysis of N_2O_5 on surfaces of sulfate aerosols was assumed to be 0.10 (*32*).

Mean temperatures within the vortex (~210 K in January, ~230 K in March) were adopted from meteorological analyses for 1991–1992 (*9*). Temperatures below the PSC threshold were assumed to occur 1 day out of 8, from 9 to 25 January (*9*). Production of Cl* by reaction of HCl and $ClNO_3$ on PSC surfaces was assumed to be rapid and stoichiometric (*5, 7*). Complete return of HNO_3 to the gas phase was assumed upon PSC evaporation, consistent with observations for 1991–92 (*26*).

Calculated changes of ClO, HCl and NO (Table 1, case A) correspond closely to observations (Fig. 6), indicating accurate simulation of rates for key processes regulating ClO after the cessation of PSCs: photochemical decomposition of HNO_3, which regenerates $ClNO_3$, and reaction of Cl with CH_4, which regenerates HCl. A study that included detailed air parcel trajectories to examine recovery from PSC processing reached similar conclusions (*33*). The integrated removal of O_3 was ~19%, similar to empirical values from the ER-2 data discussed above.

What conditions would allow high concentrations of Cl* to persist into spring, as observed in the Antarctic (*34*)? If PSC processing persisted for another month, O_3 losses would increase modestly (Table 1, case B): Photolysis of HNO_3 accelerates rapidly as the season progresses, limiting

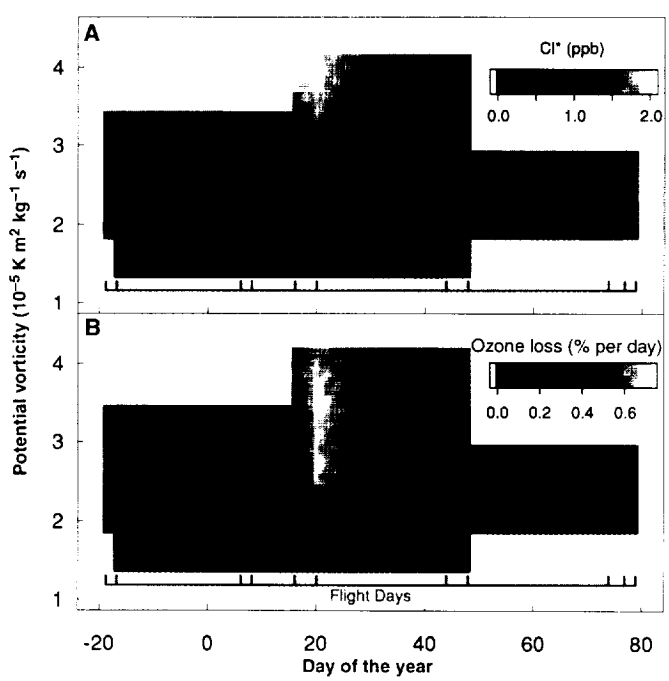

Fig. 5. (**A**) Calculated mixing ratio of Cl* (*41*) and (**B**) 24-hour mean loss rate for ozone on the $\Theta = 470 \pm 10$ K isentropic surface, plotted as a function of PV and day of the year for the Arctic polar vortex in 1991–1992. Day 1 is 1 January 1992, and negative numbers refer to 1991.

loss of O_3 after each PSC encounter. Extremely cold temperatures throughout the vortex (<195 K) in March could produce larger losses of O_3 if HNO_3 were sequestered in an aerosol phase. If HNO_3 were irreversibly removed by the sedimentation of PSCs (denitrification), Cl* would remain elevated until equinox, and O_3 losses would increase significantly (*31*, *35*) (Fig. 6 and Table 1, case C). Much of the Antarctic polar vortex is denitrified because of pervasively cold temperatures (*36*), but only sporadic denitrification has been observed in the Arctic (*26*, *36*). Large-scale denitrification could occur in the Arctic if there were an anomalously cold winter or if ice cloud formation were enhanced by increased concentrations of stratospheric H_2O. Cooling of the polar vortex could occur as a result of increasing CO_2 (*37*) or declining concentrations of O_3 (*38*). Large ozone reductions would also be expected in the Arctic without denitrification if concentrations of inorganic chlorine were to double beyond present-day values (Table 1, case D). This scenario appears unlikely if present revisions (*39*) to the Montreal Protocol of 1987 (*40*) are effective in reducing inputs of chlorocarbons and bromocarbons to the atmosphere.

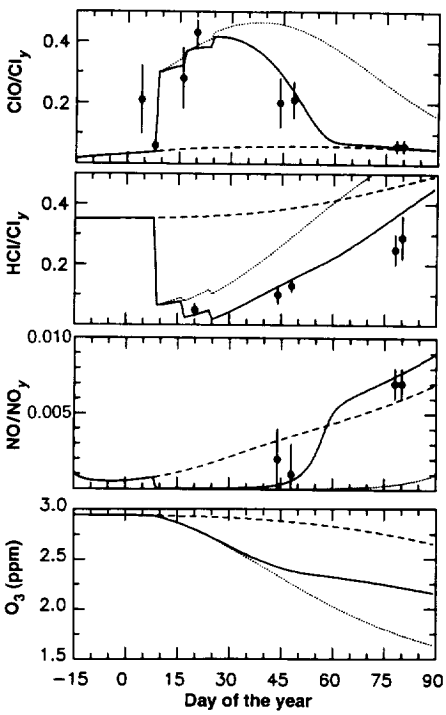

Fig. 6. Calculated seasonal evolution (day 1 corresponds to 1 January) of ClO, HCl, NO, and O_3 at noon for a hypothetical air parcel circulating at 18 km altitude, 65°N latitude, processed periodically by PSCs as described in the text. Model results for case A in Table 1 (no denitrification), case C (90% denitrification following the first PSC event), and a parcel with no PSC processing are shown by the solid, dotted, and dashed lines, respectively. Reductions in O_3 during March in the absence of PSC processing occurs because of reactions involving NO_x. Data points represent mean and standard deviation of observations for $\Theta = 470 \pm 30$ K and PV > 2.8×10^{-5} K m^2 kg^{-1} s^{-1}. Data for ClO and NO were restricted to daytime measurements (solar zenith angle < 86°). Concentrations of ClO, HCl, and NO have been normalized to either Cl$_y$ or NO$_y$ to remove the influence of small-scale atmospheric gradients.

REFERENCES AND NOTES

1. Potential temperature, Θ, is the temperature that an air parcel would reach if it were compressed adiabatically to 1000 mbar. Potential vorticity, PV, is a measure of the ratio of the absolute vorticity of a fluid layer to its depth [B. J. Hoskins, M. E. McIntyre, A. W. Robertson, *Q. J. R. Meteorol. Soc.* **111**, 877 (1985)]. For the polar stratosphere, Θ and PV are conserved typically over time scales of several weeks.
2. M. R. Schoeberl *et al.*, *J. Geophys. Res.* **94**, 16815 (1989).
3. R. J. Salawitch *et al.*, *Geophys. Res. Lett.* **17**, 561 (1990).
4. A vortex circulation forms in the stratosphere over each pole in winter. Air cools radiatively and descends within the vortex, creating steep gradients for tracers across the vortex boundary (M. Loewenstein, J. R. Podolske, K. R. Chan, S. E. Strahan, *Geophys. Res. Lett.* **17**, 477 (1990). Temperatures below the threshold for the formation of polar stratospheric clouds are pervasive in the Antarctic vortex and more localized in the Arctic (*11*).
5. D. W. Toohey *et al.*, *Science* **261**, 1134 (1993).
6. D. W. Fahey *et al.*, *Nature* **363**, 509 (1993).
7. C. R. Webster *et al.*, *Science* **261**, 1130 (1993).
8. M. H. Proffitt *et al.*, *ibid.*, p. 1150.
9. P. A. Newman *et al.*, *ibid.*, p. 1143.
10. J. C. Wilson *et al.*, *ibid.*, p. 1140.
11. M. P. McCormick, H. M. Steele, P. Hamill, W. P. Chu, T. J. Swissler, *J. Atmos. Sci.* **39**, 1387 (1982); H. M. Steele, P. Hamill, M. P. McCormick, T. J. Swissler, *ibid.* **40**, 2055 (1983).
12. O. B. Toon, P. Hamill, R. P. Turco, J. Pinto, *Geophys. Res. Lett.* **13**, 1284 (1986); P. J. Crutzen and F. Arnold, *Nature* **324**, 651 (1986); D. R. Hanson and K. Mauersberger, *Geophys. Res. Lett.* **15**, 855 (1988); D. R. Worsnop, L. E. Fox, M. S. Zahniser, S. C. Wofsy, *Science* **259**, 71 (1993).
13. M. B. McElroy, R. J. Salawitch, S. C. Wofsy, J. A. Logan, *Nature* **321**, 759 (1986).
14. S. Solomon, R. R. Garcia, F. S. Rowland, D. J. Wuebbles, *ibid.*, p. 755; W. H. Brune, D. W. Toohey, J. G. Anderson, K. R. Chan, *Geophys. Res. Lett.* **17**, 505 (1990).
15. L. T. Molina and M. J. Molina, *J. Phys. Chem.* **91**, 433 (1987).
16. K.-K. Tung, M. K. W. Ko, J. M. Rodriguez, N. D. Sze, *Nature* **322**, 811 (1986).
17. R. D. Cadle, P. Crutzen, D. Ehhalt, *J. Geophys. Res.* **80**, 3381 (1975); S. C. Wofsy, *ibid.* **83**, 364 (1978); J. F. Noxon, *ibid.* **84**, 5067 (1979); W. F. J. Evans, C. T. McElroy, I. E. Galbally, *Geophys. Res. Lett.* **12**, 825 (1985).
18. D. W. Fahey, S. R. Kawa, K. R. Chan, *Geophys. Res. Lett.* **17**, 489 (1990).
19. G. C. Toon *et al.*, *J. Geophys. Res.* **97**, 7963 (1992).
20. W. B. DeMore *et al.*, "Chemical kinetics and photochemical data for use in stratospheric modeling," *JPL Publication 92-20* (Jet Propulsion Laboratory, Pasadena, CA, 1992).
21. D. W. Toohey, J. G. Anderson, W. H. Brune, K. R. Chan, *Geophys. Res. Lett.* **17**, 513 (1990); J. G. Anderson, D. W. Toohey, W. H. Brune, *Science* **251**, 39 (1991).
22. Concentrations of BrO versus Θ from 1989 (*21*) were increased by ~10% to reflect preliminary data from 1991–1992. The relationship between Br* and Θ was developed with use of Eq. 6 and profiles of Cl*, O_3, and temperature inside the vortex for 20 January 1992. A value of Br* = 12 parts per trillion by volume (pptv) (1 pptv = 10^{-12} mole fraction in air) was used for Θ = 470 K, yielding BrO = 8.75 pptv for solar zenith angle = 86° on 20 January.
23. Total inorganic chlorine (Cl$_y$) was calculated with the relations between N_2O and the source gases CCl_3F, $C_2Cl_2F_3$, CCl_2F_2, CH_3Cl, CH_3CCl_3, and CCl_4 [J. W. Elkins *et al.*, *Eos* **73**, 106 (1992)], as described by S. R. Kawa *et al.* [*J. Geophys. Res.* **97**, 7905 (1992)].
24. We adopted cross sections from J. B. Burkholder, J. J. Orlando, and C. J. Howard [*J. Phys. Chem.* **94**, 687 (1990)], which gave Cl*/Cl$_y$ ≈ 0.75 deep inside the vortex. The use of cross sections from (*20*) [including absorption at longer wavelengths reported by W. B. DeMore and E. Tschuikow-Roux (*ibid.*, p. 5856)] gives Cl*/Cl$_y$ ≈ 1 inside the vortex. Uncertainties in Cl* have little effect on computed loss rates of O_3 because recombination depends mainly on observed daytime concentrations of ClO (Eq. 4).
25. J. W. Waters *et al.*, *Nature* **362**, 597 (1993).
26. M. Loewenstein *et al.*, in preparation.
27. M. R. Schoeberl *et al.*, *Geophys. Res. Lett.* **17**, 469 (1990); M. H. Proffitt *et al.*, *Nature* **347**, 31 (1990); D. S. McKenna *et al.*, *Geophys. Res. Lett.* **17**, 553 (1990); I. S. A. Isaksen, B. Rognerud, F. Stordal, M. T. Coffey, W. G. Mankin, *ibid.*, p. 557.
28. The Θ = 470 ± 10 K surface was chosen for analysis because it was sampled repeatedly over the winter. Surfaces characterized by higher Θ were not sampled until significant warming had occurred (February and March); surfaces with lower Θ were sampled sporadically during dives.
29. J. E. Rosenfield *et al.*, *Geophys. Res. Lett.* **17**, 345 (1990).
30. J. Collins and A. Weinheimer, personal communication.
31. R. J. Salawitch, S. C. Wofsy, M. B. McElroy, *Geophys. Res. Lett.* **15**, 871 (1988).
32. M. Mozurkewich and J. G. Calvert, *J. Geophys. Res.* **93**, 15889 (1988); J. M. Van Doren *et al.*, *J. Phys. Chem.* **95**, 1684 (1991); D. R. Hanson and A. R. Ravishankara, *J. Geophys. Res.* **96**, 17307 (1991).
33. M. R. Schoeberl *et al.*, in preparation.
34. P. M. Solomon *et al.*, *Nature* **328**, 411 (1987); W. H. Brune, J. G. Anderson, K. R. Chan, *J. Geophys. Res.* **94**, 16649 (1989).
35. W. H. Brune *et al.*, *Science* **252**, 1260 (1991).
36. D. W. Fahey *et al.*, *Nature* **344**, 321 (1990).
37. Intergovernmental Panel on Climate Change, *Climate Change: The IPCC Scientific Assessment*, J. T. Houghton, G. J. Jenkins, J. J. Ephraums, Eds. (Cambridge Univ. Press, Cambridge, 1990), chap. 5.
38. "Scientific assessment of ozone depletion: 1991," *World Meteorological Organization Rep. No. 25* (1991), chap. 7.
39. Montreal Protocol on the Substances that Deplete the Ozone Layer as Adjusted and Amended by the 4th Meeting of the Parties, Copenhagen, Denmark, 19 to 21 November 1992, United Nations Environment Program.
40. M. B. McElroy and R. J. Salawitch, *Science* **243**, 763 (1989).
41. The apparently detached parcel with high Cl* in early January (2.1×10^{-5} < PV < 2.7×10^{-5} K m^2 kg^{-1} s^{-1}) is an artifact; small-scale features with high ClO and low N_2O, characteristic of air with high PV from deep inside the vortex, alternated with low-ClO, high-N_2O air over 10- to 100-km scales. Meteorological fields of potential vorticity are typically unable to resolve features on this scale (*2*).

42. Supported by grants from the National Aeronautics and Space Administration's High-Speed Research Program and Upper Atmosphere Program and by the National Science Foundation's Atmospheric Chemistry Program. Helpful discussions with S. R. Kawa and A. Weaver are gratefully acknowledged. We thank L. M. Avallone and D. W. Toohey for helpful discussions and for making data on ClO and BrO available.

26 February 1993; accepted 13 July 1993